REPORT DOCUMENTAT

1. AGENCY USE ONLY (Leave blank)	2. REPORT DATE	3. REPORT TYPE AND DATES COVERED
	January 1994	

4. TITLE AND SUBTITLE

Measured Channel Parameters for the Disturbed Wide-Bandwidth HF Channel

5. FUNDING NUMBERS

DAAB07-93-C-H651

6. AUTHOR(S)

Christopher A. Nissen, Phillip A. Bello

7. PERFORMING ORGANIZATION NAME(S) AND ADDRESS(ES)

The MITRE Corporation
202 Burlington Road
Bedford, MA 01730-1420

8. PERFORMING ORGANIZATION REPORT NUMBER

MP 94B0000006

9. SPONSORING/MONITORING AGENCY NAME(S) AND ADDRESS(ES)

U.S. Army

10. SPONSORING/MONITORING AGENCY REPORT NUMBER

11. SUPPLEMENTARY NOTES

12a. DISTRIBUTION/AVAILABILITY STATEMENT

Approved for public release; distribution unlimited.

12b. DISTRIBUTION CODE

13. ABSTRACT (Maximum 200 words)

Recent measurements have been made of the wideband HF (WBHF) channel impulse response over a high-latitude auroral path using the MITRE experimental WBHF test facility. A nominal instantaneous bandwidth of 1 MHz was used for the majority of the tests. These tests took place from 14 March through 1 April 1992 over a path from Söndrestrom AFB, Greenland to Bedford, Massachusetts, a distance of approximately 3100 km. The measurements were made using a direct-sequence pseudo-noise (DSPN) channel probe with a chip rate of 1024 ksamples per second. Channel impulse response samples at increments of 500 nanoseconds in delay were derived by correlating the received signal with a set of local DSPN references uniformly spaced in delay over a delay range of 2 ms. The channel was sampled in this fashion at a rate of up to 62.5 samples per second, resulting in the ability to observe Doppler spreads and shifts of up to 31.25 Hz. From these measurements the channel scattering function, rms (2σ) Doppler spread, rms (2σ) Delay spread, Doppler shift, and rms (2σ) spread factor were calculated. In addition, for the first time, the impulse response correlation along the delay axis was calculated. These latter measurements support the use of an uncorrelated scattering hypothesis in modeling the disturbed WBHF channel.

14. SUBJECT TERMS

wideband HF, channel impulse response, correlation, measurements, Doppler spread

15. NUMBER OF PAGES

18

16. PRICE CODE

17. SECURITY CLASSIFICATION OF REPORT	18. SECURITY CLASSIFICATION OF THIS PAGE	19. SECURITY CLASSIFICATION OF ABSTRACT	20. LIMITATION OF ABSTRACT
Unclassified	Unclassified	Unclassified	Unlimited

Measured Channel Parameters for the Disturbed Wide-Bandwidth HF Channel

MP 94B0000006
January 1994

Christopher A. Nissen
Phillip A. Bello

MITRE
Bedford, Massachusetts

Measured Channel Parameters for the Disturbed Wide-Bandwidth HF Channel

MP 94B0000006
January 1994

Christopher A. Nissen
Phillip A. Bello

Contract Sponsor U.S. Army
Contract No. DAAB07-93-C-H651
Project No. 8632B
Dept. D053/D050

MITRE

Bedford, Massachusetts

Department Approval: 

MITRE Project Approval: 

ABSTRACT

Recent measurements have been made of the wideband HF (WBHF) channel impulse response over a high-latitude auroral path using the MITRE experimental WBHF test facility. A nominal instantaneous bandwidth of 1 MHz was used for the majority of the tests. These tests took place from 14 March through 1 April 1992 over a path from Söndrestrom AFB, Greenland to Bedford, Massachusetts, a distance of approximately 3100 km. The measurements were made using a direct-sequence pseudo-noise (DSPN) channel probe with a chip rate of 1024 ksamples per second. Channel impulse response samples at increments of 500 nanoseconds in delay were derived by correlating the received signal with a set of local DSPN references uniformly spaced in delay over a delay range of 2 ms. The channel was sampled in this fashion at a rate of up to 62.5 samples per second, resulting in the ability to observe Doppler spreads and shifts of up to 31.25 Hz. From these measurements the channel scattering function, rms (2σ) Doppler spread, rms (2σ) Delay spread, Doppler shift, and rms (2σ) spread factor were calculated. In addition, for the first time, the impulse response correlation along the delay axis was calculated. These latter measurements support the use of an uncorrelated scattering hypothesis in modeling the disturbed WBHF channel.

ACKNOWLEDGMENTS

The authors would like to extend thanks to all the people that participated in the experiment preparation and execution. We would especially like to thank the equipment operators including Paul Fine, Marc Richard, Marcel Jussaume, and Joel Freedman for the long hours and dedication they displayed. We would also like to thank Ed Piekielek for the uploading and copying of the data tapes.

TABLE OF CONTENTS

LIST OF ILLUSTRATIONS

SECTION 1
BACKGROUND

MITRE [1]–[4], NRL [5]–[7], and SRI [8], have conducted WBHF propagation measurements in order to characterize the WBHF channel. The present measurements add to this growing data base. Prior measurements of disturbed channels by NRL and SRI used bandwidths of 31 or 20 kHz, respectively, substantially smaller than 1 MHz, the bandwidth used in our measurements. Thus,the present experiments have allowed examination of the impulse response statistics of disturbed channels at a resolution of the order of 1 microsecond.

The scattering function is a concept that arises in modeling of random time-variant scatter-type channels. Strictly speaking, it is associated with the idealized wide-sense-stationary uncorrelated-scattering (WSSUS) channel model [9]. In this model, the channel is represented by a continuum of uncorrelated statistically stationary fluctuating scatterers. The scattering function is proportional to the power density spectrum of these scatterers as a function of path delay.

An important question explored in this paper, for the first time, is the validity of the uncorrelated-scattering (US) property for the WBHF channel. The measured impulse response is the convolution of the WBHF channel impulse response with the impulse response of a composite terminal equipment filter. This equipment filter is composed of the cascade of any filters in the transmitter and receiver with a filter representing the DSPN chip pulse. Due to the smearing operation of the equipment filter, the measured impulse response will no longer be US even if the WBHF channel were WSSUS. However one may show that if the channel were WSSUS, the correlation between impulse response fluctuations at two different delay values separated by T microseconds is proportional to the autocorrelation function of the equipment filter at the lag T. Thus it is still possible to explore the US property to within the resolution of the equipment filter.

SECTION 2
DATA COLLECTION AND PROCESSING

The channel was probed by a 500-watt filtered binary PSK DSPN signal with a chip rate of 1.024 MHz. A transmitter filter with a bandwidth of 1 MHz was used. At the receiver, the passband was controlled primarily by digital filtering at a sampling rate of 8192 kHz with subsequent downsampling to 2048 complex ksamples per second. The resulting equivalent IF passband was flat to 0.1 dB over 1 MHz but had negligible transmission outside a 2 MHz band. Thus, the composite equipment filter was essentially the same as the 1 MHz bandlimiting filter at the transmitter.

The sampled waveform was next processed by a narrowband interference excisor, and correlated over 4096 taps, each spaced approximately 500 nanoseconds apart resulting in a total delay window of approximately 2 ms. Each correlator includes an integrate and dump (I&D) circuit, the outputs of which are used to produce estimates of the channel impulse response. For these experiments, a channel measurement consisted of a series of 512 impulse response measurements taken at sampling rates of 62.5, 31.25, or 15.625 samples/second resulting in channel measurement durations of 8.192, 16.384, and 30.797 seconds, respectively. At the very beginning of the probe experiment, before data collection began, the delay of the PN sequence was adjusted such that the majority of the impulse response was positioned in the correlator window. The resulting channel probe data was processed off-line after completion of the testing. An approximation of the scattering function was calculated from the family of 512 impulse response measurements by averaging the squared magnitude of four 128-point discrete Fourier transforms of the impulse response at each value of delay and smoothing in both the delay and Doppler dimensions by convolving with windows. A 25-point Kaiser-Bessel window was used in the Doppler domain and a 45-point Kaiser-Bessel window was used in the delay domain. The resulting calculation is referred to here as the scattering function estimate.

SECTION 3
RESULTS

The above procedure was used to determine the scattering function for each of the channel measurements recorded during the tests. The rms (2σ) Doppler spread, rms (2σ) Delay spread, and Doppler shift values were then compiled to form a database of measured channel conditions during the testing interval. Figure 1 is an example scattering function and the associated contour plot for the channel measurement taken on 1 April 1992 at 0734 UTC at a center frequency of 15.5 MHz. Here, the contour plot is shown to illustrate the fine details regarding the location of the major propagation modes in terms of delay and Doppler axis values. The levels of the contour were chosen to subdivide the power axis into 20 equal divisions. Note the presence of several modes, each consisting of significant signal energy. The rms Doppler spread for this example is 7.5 Hz, the rms multipath spread is around 100 microseconds, and the mean Doppler shift is 6.6 Hz. The standard oblique-incidence ionogram that was recorded using an LFMCW chirpsounder, and taken in conjunction with the WBHF channel measurement, is shown in Figure 2. Note that although there is 300–400 microseconds of delay spread evident on the oblique ionogram at the center frequency, the scattering function processing of the WBHF channel probe indicates that, using the rms metric on delay spread, only approximately 100 microseconds of spread is significant in terms of received energy. An analysis of the correlation between the complex signal components at each tap is performed on this channel measurement later in this paper.

Figures 3(a)–3(d) present plots of the cumulative distribution functions of the rms Doppler spread, Doppler shift magnitude, rms delay spread, and spread factor (product of multipath spread by Doppler spread) values for the entire WBHF channel probe database obtained during the tests. After removing channel probes which had significant signal contributions from more than one propagation mode, there were approximately 100 channel probe measurements in the database. The multi-mode probes were not used in the statistical compilation since the inclusion of multiple modes would, by definition, be invalid for any of the spread and shift statistics.

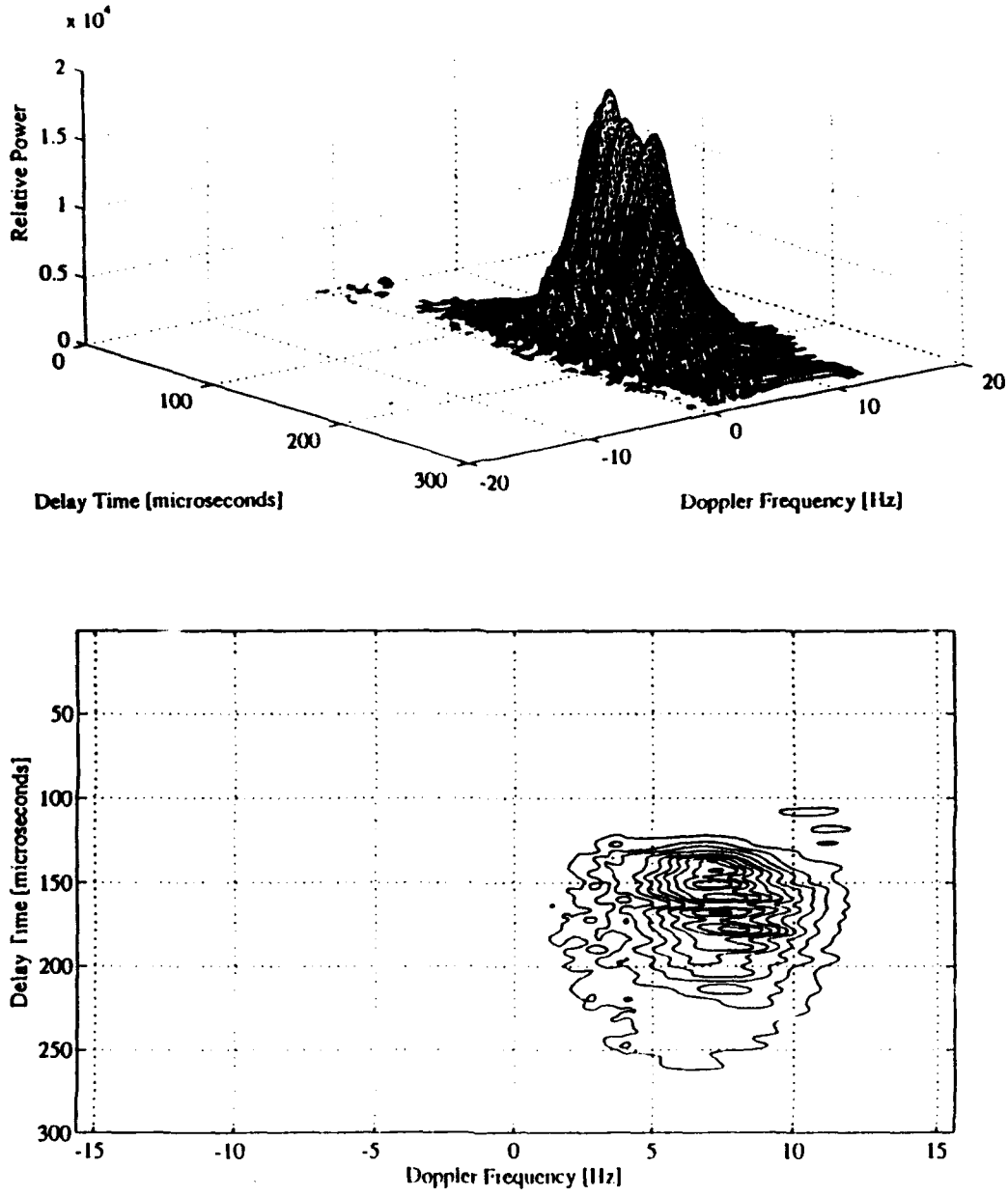

Figure 1 Disturbed Channel Scattering Function for WBHF Channel Measurement (made on 1 April at 0734 UTC at a center frequency of 15.5 MHz).

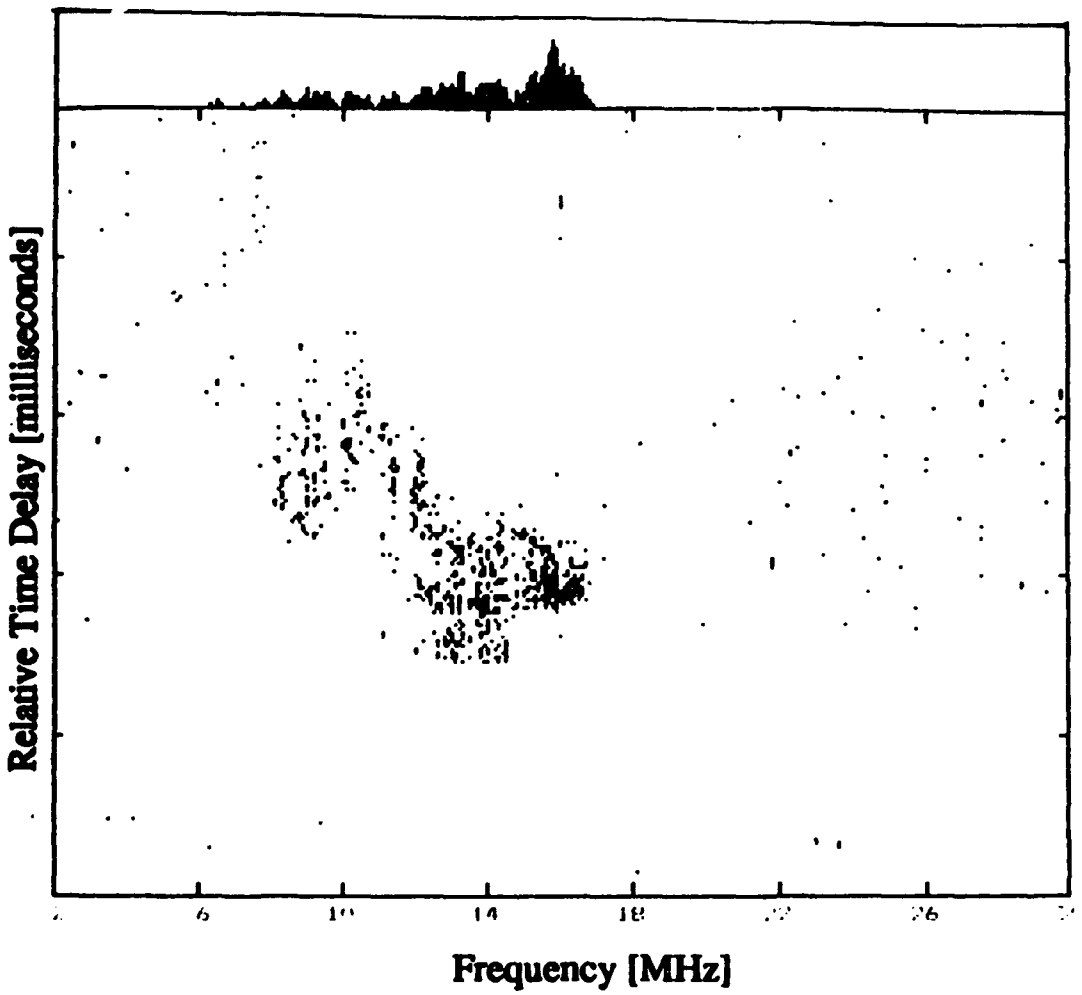

Figure 2 Oblique Incidence Ionogram Beginning at 0735 UTC.

Figure 3(a) shows the median value of rms Doppler spread observed during the tests was 5 Hz, with 10th and 90th percentile values of 1.75 and 13 Hz, respectively. The largest value observed was 17 Hz. Extensive use was made of geophysical and solar-terrestrial conditions as reported by the Space Environment Services Laboratory (SESL) during the tests. There was a noticeable correlation between large solar flares on 15 March and 1 April and the measured wideband channel conditions. The largest value of rms Doppler spread was measured on 15 March and it is believed that this disturbance is directly attributable to the major M-class solar flare observed on that day. Although the testing period could be characterized as relatively "quiet" to "unsettled" except for the events around 14, 15 March and 1 April, there was an overall "floor", or average value during periods of quiet geomagnetic activity of roughly 2 Hz rms Doppler spread. Even this value represents mildly disturbed conditions relative to the nominal Doppler spread of less than 0.4 Hz recorded on mid-latitude paths[3].

The Doppler shifts of the main propagation modes recorded by the channel probes were generally small. Figure 3(b) shows the cumulative distribution of the Doppler shift magnitude for the database. Here the median value is seen to be roughly 0.5 Hz; the 10th percentile indicated no shift; and the 90th percentile shift is just below three Hertz. Increased shift values were noted on 1 April; the date of the disturbed magnetic conditions when there were several consecutive positive Doppler shifts of relatively large magnitude, implying a pronounced "drift" velocity of the ionosphere.

Figure 3(c) is a plot of the cumulative distribution of the rms delay spread. The median value is seen to be roughly 100 microseconds; the 10th percentile point was found to be 17 microseconds; the 90th percentile point is slightly larger than 400 microseconds. Values of delay spread were moderately large during unsettled to active periods of geomagnetic disturbances. Large delay spread values are indicative of disturbed channels commonly described as "spread F" or "auroral F", so termed because of the spread easily identified on the F-layer traces of a standard oblique ionogram. However, examples were noted where the oblique incidence sounder either did not show propagation support when, in fact there was support obvious from the wideband channel probe, or the amount of spread indicated on the ionogram was misleading since the signal energy within an rms bandwidth was significantly lower. It was again noted that the largest values of delay spread were recorded on 1 April.

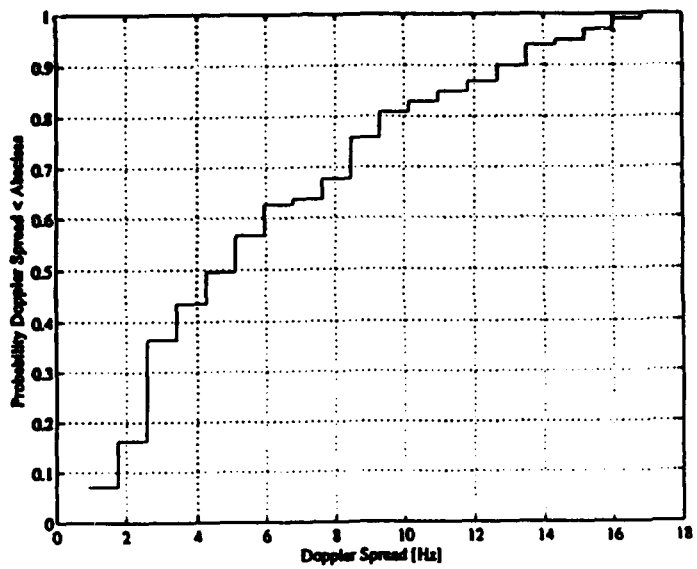

3-a

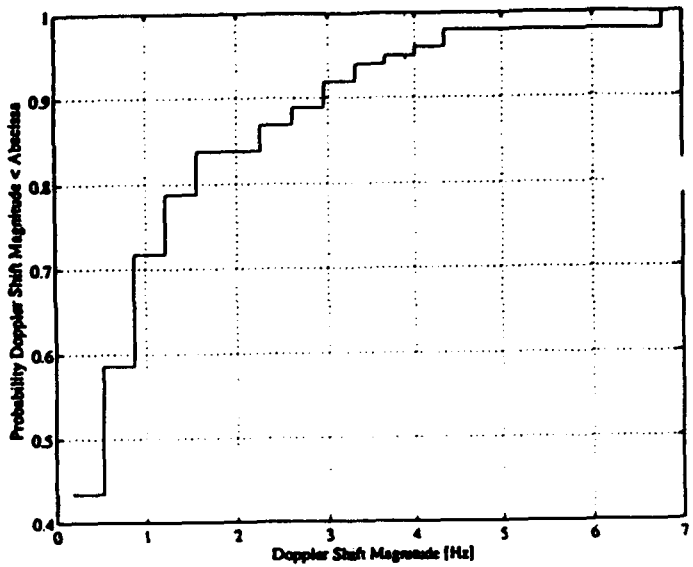

3-b

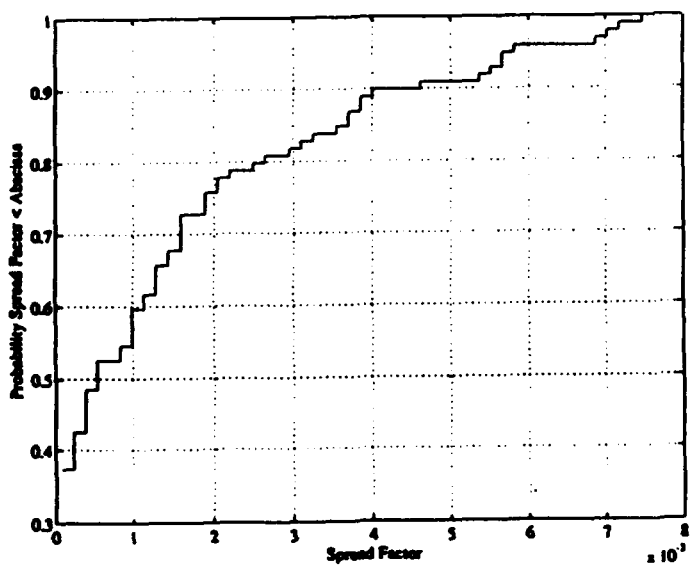

3-d

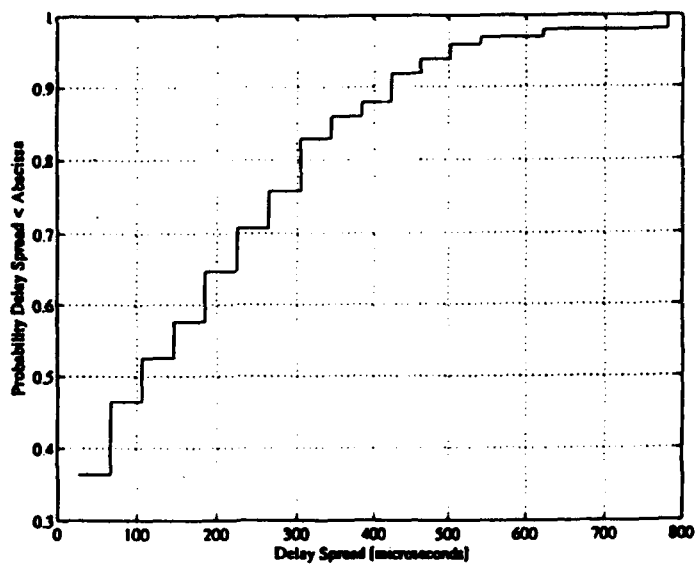

3-c

Figure 3 Cumulative Distribution Functions of Doppler Spread, Doppler Shift, Delay Spread, and Spread Function.

Figure 4 shows a scatter plot of the Doppler and delay spread for each experiment. The product of rms delay spread and rms Doppler spread is called the rms *spread factor*. Kailath [10] showed that a random time-varying channel becomes nonmeasurable when the total spread factor exceeds 1, where spread factor was defined as the product of *total* Doppler spread by *total* delay spread. Bello [11] sharpened this criterion by showing that the channel becomes nonmeasureable when the *area* spread factor is greater than 1, where the area spread factor is the area occupied by the scattering function over the delay-Doppler plane. A more practical consideration is the fact that the output SNR of the channel measurement at the correlator output is equal to the input SNR to the receiver divided by the spread factor. The spread factor has been calculated for each of the channel measurements in the database. The cumulative distribution of the values is shown in Figure 3(d). Because this figure was plotted to show the common range of values, the absolute minimum value of 7.4×10^{-6} cannot be read. The absolute largest value was 7.5×10^{-3}; the median was 5.3×10^{-4}; the 10th percentile was less than 10^{-4}; and the 90th percentile was 6×10^{-3}. Note this figure indicates that 60 percent of the time, the rms spread factor was roughly three orders of magnitude below one. The values of multipath, Doppler spread, and spread factors are comparable to those obtained by Wagner for a near vertical incidence Auroral HF channel [12], although our Doppler spreads and spread factors are somewhat larger.

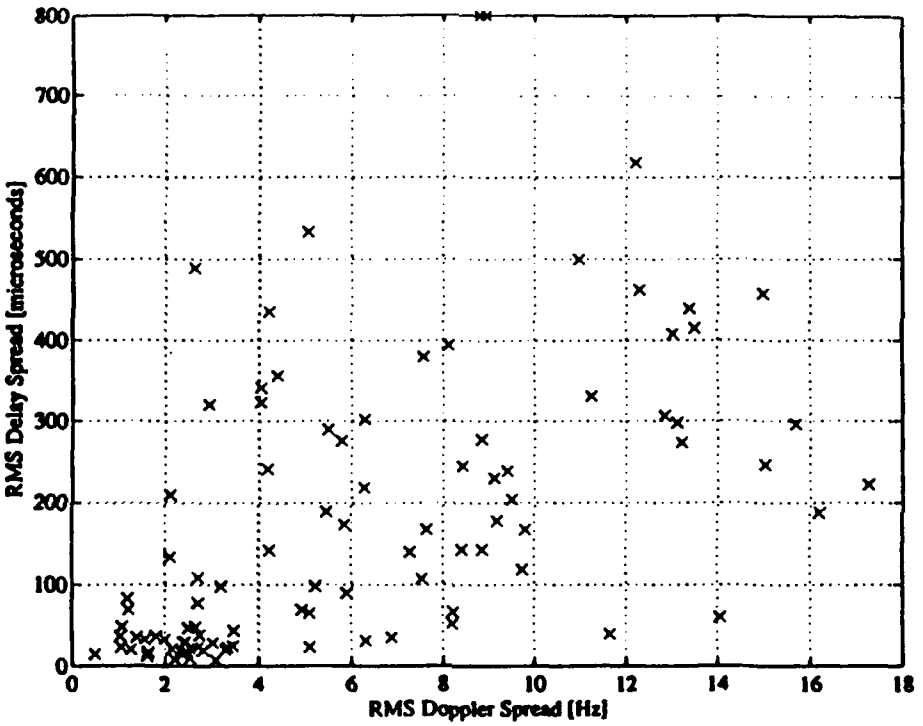

Figure 4 Scatter Plot of Delay Spread vs. Doppler Spread.

SECTION 4
CORRELATION COEFFICIENT OF CHANNEL MEASUREMENTS

The normalized correlation coefficient matrix, $R(m,p)$, is the matrix whose element (m,p) is:

$$R(m,p) = \frac{\sum_k \left\{ \left(h^*(kT, m\Delta) - \mu_{(m)} \right) \left(h\left(kT, (m+p)\Delta\right) - \mu_{(m+p)} \right) \right\}}{\sqrt{\left(\sum_k \left| h(kT, m\Delta) - \mu_{(m)} \right|^2 \right) \left(\sum_k \left| h(kT, (m+p)\Delta) - \mu_{(m+p)} \right|^2 \right)}}$$

where h is the complex channel impulse response measured over kT seconds and N taps, each spaced by Δ seconds and indexed by m, and μ_m is the sample mean of the impulse response at the delay $m\Delta$. The time displacement, or time lag, is represented by the quantity $m + \rho$. The tap spacing, Δ, was 0.488 microseconds for these measurements and T was 16.384 seconds.

An observation of N taps is denoted using the correlation coefficient matrix as:

$$R(m,p) = \begin{bmatrix} 1 & \rho_{21} & \rho_{31} & \cdots & \rho_{N1} \\ \rho_{12} & 1 & \rho_{32} & \cdots & \rho_{N2} \\ \rho_{13} & \rho_{23} & \cdot & \cdots & \rho_{N3} \\ \cdot & \cdot & \cdot & \cdot & \cdot \\ \rho_{1N} & \cdot & \cdot & \cdots & 1 \end{bmatrix}$$

where ρ_{mp} is the covariance of the m'th tap at the p'th lag normalized by ρ_{mp} where $m = p$. The matrix is symmetric; thus, by examining the diagonals in either the upper or lower triangles, one can see how quickly, in terms of the number of taps, the signal becomes uncorrelated. The correlation coefficient matrix was calculated for the channel impulse response measurement examined above in the discussion of the channel scattering function. The impulse response has significant magnitude between taps 200 and 400. $R(m,p)$ was then calculated using taps 200–399 resulting in the 200 × 200 correlation coefficient matrix. Figure 5 presents the estimated correlation between impulse response samples as a function of the delay separation in microseconds obtained from the correlation matrix by averaging the values in each diagonal (each diagonal corresponding to a fixed delay separation between taps). The correlation between taps is seen to drop to small values within a few microseconds. The results presented using this example are representative of several such correlation analyses that were performed.

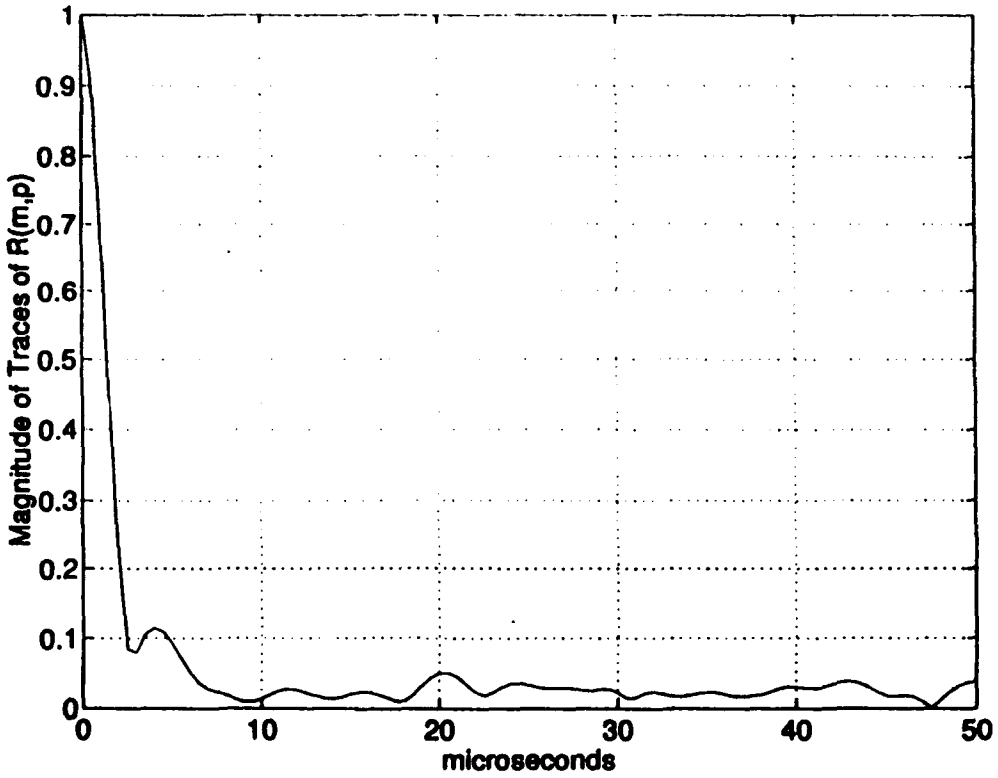

Figure 5 Average Value of the Magnitude of the Correlation Coefficient Matrix Traces.

SECTION 5
SUMMARY

High-latitude HF-channel 1 MHz bandwidth impulse responses were measured at several frequencies over a 3100-km path from Söndrestrom AFB, Greenland, to Bedford, Massachusetts, from 14 March–1 April 1992. From these measurements, computations were made of delay-Doppler scattering functions, rms (2σ) Doppler spreads, Doppler shifts, rms (2σ) delay spreads, rms (2σ) spread factors, and impulse response correlations vs. path delay. The largest value, 90th percentile, and 10th percentile of the rms Doppler spread, Doppler shift, rms delay spread and rms spread factor were (16.8 Hz, 1.75 Hz, 13.0 Hz, resp.) , (7.0 Hz, $<<1$ Hz, 3 Hz, resp.), (780 μs, 17 μs, 400 μs, resp.), and (7.5×10^{-3}, $< 10^{-4}$, 6×10^{-3}, resp.), respectively. The ionosphere was mildly disturbed except for major solar flares on 14, 15 March and 1 April. Larger Doppler spreads and shifts can be correlated to these events. Impulse response correlations vs. path delay drop to small values for delay changes of the order of the equipment filter impulse response autocorrelation function, supporting the hypothesis of an uncorrelated scattering channel model.

LIST OF REFERENCES

1. B. D. Perry and R. Rifkin, "Measured Wideband HF Mid-Latitude Channel Characteristics," *MITRE Technical Report MTR10790, Bedford, MA* (June 1991). (See also "Measured Wideband HF Mid-Latitude Ionospheric Channel Characteristics", *1989 IEEE Military Communications Conference (MILCOM'89)*, (October 1989), 4[illegible]1–8).

2. R. Rifkin and B. D. Perry, "Bandwidth Effects of Signal Fading for the Mid- Latitude HF Channel," *1990 IEEE Military Communications Conference, Monterey, California* . **Vol. 3** (October 1990), 60.4.1–8.

3. M. I. Clune, P. B. Fine, J. N. Freedman, C. A. Nissen, and B. D. Perry, "Delay and Doppler Spreading Characteristics of the Wide-Bandwidth HF Channel," *IEE Conference Publication for the Fifth International Conference on HF Radio Systems and Techniques* (Edinburgh, U.K., July 1991), Also MITRE Document M91-29.

4. B. D. Perry and R. Rifkin, "Long-Term Wide-Bandwidth Channel Characteristics and Bandwidth-Dependent Fading for a Mid-Latitude HF Path," *IEE Conference Publication for the Fifth International Conference on HF Radio Systems and Techniques* (Edinburgh, U.K., July 1991).

5. L. S. Wagner, J. A. Goldstein, and W. D. Meyers, "Wideband Probing of the Trans-auroral HF Channel," *IEEE Military Communication Conference Proceedings* **Vol.3** (October 1987).

6. L. S. Wagner, J. A. Goldstein, and W. D. Meyers, "Wideband Probing of the Trans-auroral Channel: Solar Minimum," *Radio Science* **Vol.23, No.4** (July-August 1988), 555–568.

7. L. S. Wagner and J. A. Goldstein, "High Resolution Probing of the HF Ionospheric Skywave Channel: F2 Layer Results," *Radio Science* **Vol.20, No.3** (1985), 287–302.

8. Roy P. Basler, Gary H. Price, Roland T. Tsunoda, and Terrence L. Wong, "Ionospheric Distortion of HF Signal," *Radio Science* **Vol.23, No.4** (July-August 1988), 561–579.

9. P. A. Bello, "Characterization of Randomly Time-Variant Linear Channels," *IEEE Trans. on Comm. Systems* **Vol. CS-11, No. 4** (December 1963), 360–393.

10. Kailath, T., "Sampling Models for Linear Time-Variant Filters," *M.I.T. Research Lab. of Electronics, Cambridge MA, Rept. No. 352* (May 25, 1959).

11. Phillip A. Bello, "Measurement of Random Time-Variant Linear Channels," *IEEE Trans. on Info. Theory* **Vol. IT-5, No. 4** (July 1969), pages 469–475.

12. L. S. Wagner, "Channel Spread Parameters for the Near-Vertical-Incidence Auroral HF Channel," *Report NRL-NR-5554 - 94-7499, Naval Research Labs, Washington, DC* (February 1994).